Cancer Treatment and Research Communications 32 (2022) 100583

Contents lists available at ScienceDirect

Cancer Treatment and Research Communications

journal homepage: www.sciencedirect.com/journal/cancer-treatment-and-research-communications

Dynamic ^{18}F-FET PET/CT to differentiate recurrent primary brain tumor and brain metastases from radiation necrosis after single-session robotic radiosurgery

Winna Lim [a,1], Gueliz Acker [b,c,d,1], Juliane Hardt [e,f,g], Markus Kufeld [c,h,i], Anne Kluge [c,i], Winfried Brenner [j,2], Alfredo Conti [k,l], Volker Budach [c,i], Peter Vajkoczy [b,c], Carolin Senger [c,i], Vikas Prasad [j,m,*]

[a] Department of Radiology, Charité – Universitätsmedizin Berlin, Corporate member of Freie Universität Berlin, Humboldt-Universität zu Berlin, and Berlin Institute of Health, Augustenburger Platz 1, Berlin 13353, Germany
[b] Department of Neurosurgery, Charité – Universitätsmedizin Berlin, Corporate member of Freie Universität Berlin, Humboldt-Universität zu Berlin, and Berlin Institute of Health, Charitéplatz 1, Berlin 10117, Germany
[c] Charité CyberKnife Center, Charité – Universitätsmedizin Berlin, Corporate member of Freie Universität Berlin, Humboldt-Universität zu Berlin, and Berlin Institute of Health, Augustenburger Platz 1, Berlin 13353, Germany
[d] BIH Academy, Clinician Scientist Program, Berlin Institute of Health at Charité – Universitätsmedizin Berlin, Charitéplatz 1, Berlin 10117, Germany
[e] Department of Biometry, Epidemiology and Information Processing, WHO Collaborating Center for Research and Training for Health in the Human-Animal-Environment Interface, University of Veterinary Medicine (Foundation) Hannover (TiHo), Buenteweg 2, Hanover 30559, Germany
[f] Institute of Biometry and Clinical Epidemiology, Charité – Universitätsmedizin Berlin, Corporate member of Freie Universität Berlin, Humboldt-Universität zu Berlin, and Berlin Institute of Health, Germany
[g] Medical Information Management, Faculty of Information and Communication, University of Applied Sciences Hannover, Germany
[h] European Radiosurgery Center Munich, Max Lebsche-Platz 31, Munich 81377, Germany
[i] Department of Radiation Oncology, Charité – Universitätsmedizin Berlin, Corporate member of Freie Universität Berlin, Humboldt-Universität zu Berlin, and Berlin Institute of Health, Augustenburger Platz 1, Berlin 13353, Germany
[j] Department of Nuclear Medicine, Charité – Universitätsmedizin Berlin, Corporate member of Freie Universität Berlin, Humboldt-Universität zu Berlin, and Berlin Institute of Health, Augustenburger Platz 1, Berlin 13353, Germany
[k] Department of Biomedical Science and Neuromotor Sciences DIBINEM, Alma Mater Studiorum - Università di Bologna, Dipartimento di Scienze Biomediche e Neuromotorie (DIBINEM), Via Altura 3, 40139 29 Bologna (BO), Italy
[l] IRCCS Istituto delle Scienze Neurologiche di Bologna, Via Altura 3, Bologna (BO) 40139, Italy
[m] Department of Nuclear Medicine, University Hospital of Ulm, Ulm 89070, Germany

ARTICLE INFO

Keywords:
Radiation necrosis
Robotic radiosurgery
Cyberknife
^{18}F-FET-PET/CT
Dynamic ^{18}F-FET-PET/CT
Amino acid PET

ABSTRACT

Objective: Cyberknife robotic radiosurgery (RRS) provides single-session high-dose radiotherapy of brain tumors with a steep dose gradient and precise real-time image-guided motion correction. Although RRS appears to cause more radiation necrosis (RN), the radiometabolic changes after RRS have not been fully clarified. ^{18}F-FET-PET/CT is used to differentiate recurrent tumor (RT) from RN after radiosurgery when MRI findings are indecisive. We explored the usefulness of dynamic parameters derived from ^{18}F-FET PET in differentiating RT from RN after Cyberknife treatment in a single-center study population.

Methods: We retrospectively identified brain tumor patients with static and dynamic ^{18}F-FET-PET/CT for suspected RN after Cyberknife. Static (tumor-to-background ratio) and dynamic PET parameters (time-activity curve, time-to-peak) were quantified. Analyses were performed for all lesions taken together (TOTAL) and for brain metastases only (METS). Diagnostic accuracy of PET parameters (using mean tumor-to-background ratio

Abbreviations: p.p., percentage points; RN, radiation necrosis; RT, recurrent tumor; ^{18}F-FET-PET/CT, (O-(2-[F]-fluoroethyl)-l-tyrosine (F-FET) - positron emission tomography / computed tomography; cMRI, cranial magnetic resonance imaging; RRS, robotic radiosurgery; SRS, stereotactic radiosurgery; TBR, tumor-to-background ratio; TTP, time to peak; TAC, time activity curve; ROC, receiver-operating-characteristics; WBRT, whole brain radiotherapy; Gy, Gray.

* Corresponding author at: Department of Nuclear Medicine, Charité – Universitätsmedizin Berlin, Corporate member of Freie Universität Berlin, Humboldt-Universität zu Berlin, and Berlin Institute of Health, Augustenburger Platz 1, Berlin 13353, Germany.
E-mail address: vikas.prasad@uniklinik-ulm.de (V. Prasad).

[1] These authors contributed equally to this work.
[2] German Cancer Consortium (DKTK) Campus Berlin, Germany

https://doi.org/10.1016/j.ctarc.2022.100583

Available online 3 June 2022

>1.95 and time-to-peak of 20 min for RT as cut-offs) and their respective improvement of diagnostic probability were analyzed.
Results: Fourteen patients with 28 brain tumors were included in quantitative analysis. Time-activity curves alone provided the highest sensitivities (TOTAL: 95%, METS: 100%) at the cost of specificity (TOTAL: 50%, METS: 57%). Combined mean tumor-to-background ratio and time-activity curve had the highest specificities (TOTAL: 63%, METS: 71%) and led to the highest increase in diagnosis probability of up to 16% p. – versus 5% p. when only static parameters were used.
Conclusions: This preliminary study shows that combined dynamic and static ^{18}F-FET PET/CT parameters can be used in differentiating RT from RN after RRS.

1. Introduction

1.1. Robotic radiosurgery – CyberKnife®

About 8–10% of adult cancer patients in the United States will develop brain metastases - with lung cancer, breast cancer, and melanoma being the most common underlying primaries [1,2]. Stereotactic radiosurgery (SRS) is especially suitable for patients with one to four smaller (<4 cm) brain metastases [2,3]. When multiple metastases, particularly large and non-spherical tumors, are present, robotic radiosurgery has been proven effective regarding patient survival and local tumor control [4].

The steep dose gradient between tumor and normal tissue in radiosurgery allows precise dose delivery to the target lesion while sparing healthy brain tissue and critical structures. Robotic radiosurgery (RRS) is a non-invasive treatment option that combines non-coplanar and non-isocentric beam delivery with target tracking and motion compensation. These features ensure excellent submillimeter treatment precision for the elimination of a wide variety of cancers [5,6]. Although RRS' unique technology has been shown to be efficient in the treatment of brain malignancies [7–9], the mode of action and radiobiology remain to be fully elucidated [10,11]. The 5 R's of radiobiology - Repair, Repopulation, Redistribution, Reoxygenation, Radiosensitivity – known to determine the effect of conventional radiotherapy might apply here too [12], but other mechanisms seem also to play a major role in the radiobiological mechanism of action of radiosurgery, such as anti-tumor immunity and vascular damage [10]. Importantly, the high single radiation dose administered in SRS has been shown to be associated with higher rates of radiation necrosis (RN), which can appear months or even years after radiation [13].

Pseudoprogression is an important concern in the radiosurgical community because it is challenging to differentiate from true tumor progression in routine follow-up imaging [14], to which the unique underlying radiobiological mechanisms just might contribute. A close patient follow-up after treatment is needed to ensure early detection of tumor recurrence. Thus, in the follow-up of patients after radiosurgery, it is important to differentiate such radiation-induced brain damage from recurrent tumor (RT), which hitherto remains a major challenge. Both conditions occur in previously irradiated area and its immediate surroundings, present with a range of similar symptoms, and have similar imaging features in follow-up cranial magnetic resonance imaging (cMRI) [15]. Their therapeutic consequences though, are different. Oral corticosteroid treatment is the first choice in patients with radiation necrosis. In patients with steroid-resistant symptoms, VEGF is prescribed [16]. Less commonly used alternative therapeutic options include anticoagulants, hyperbaric oxygen therapy, laser interstitial thermal therapy, and, as a last resort, surgical resection. In patients with recurrent tumor, individualized management decided upon by an interdisciplinary board is warranted.

1.2. Amino acid ^{18}F-FET-PET/CT scan

Supplementary functional imaging with positron emission tomography (PET) and computed tomography (CT) is used to resolve inconclusive cases [17,18]. Amino acid PET with a modified fluorine as tracer (O-(2-[^{18}F]-fluoroethyl)-l-tyrosine (^{18}F-FET) has been shown to be helpful in solving this issue in the follow-up of brain tumor patients after SRS. For dynamic ^{18}F-FET-PET/CT parameters, diagnostic accuracies with sensitivities of 69% to 95% and specificities of 83% to 93% have been reported for brain metastases [19–23] and sensitivities of 80% to 100% and specificities of 75% to 100% for recurrent glioma [24–28]. However, a longer PET acquisition time is required to obtain the dynamic parameters in addition to standard static single-point PET imaging, which precludes its routine use in the clinical setting.

1.3. Aim

To the best of our knowledge, dynamic ^{18}F-FET-PET/CT has not been specifically investigated in the follow-up of patients with brain tumors treated with RRS only. Since the radiobiology of SRS appears to be unique, which have a steeper dose gradient, the morphological changes after robotic radiosurgery might also look different. Thus, our aim was to perfrom an explorative retrospective study using existing 'real world' data to analyze whether dynamic ^{18}F-FET-PET/CT parameters are applicable and could improve diagnostic accuracy in this specific patient group treated with robotic radiosurgery.

2. Materials and methods

2.1. Study population

We conducted a retrospective study of diagnostic accuracy in patients treated at the Charité CyberKnife Center. The Standards for Reporting Studies of Diagnostic Accuracy (STARD) were used as guidelines [29]. This study was approved by the local ethics committee (approval code EA4/222/17).

The patient database of the Charité Cyberknife Center was searched for brain tumor patients who underwent RRS and had suspected tumor recurrence with the differential diagnosis of radiation necrosis on cMRI. Both primary and secondary brain tumors were included, while resection cavities were excluded from the analysis. Furthermore, patients who subsequently underwent only static PET examinations were excluded, as only patients with acquisition of both static and dynamic parameters in ^{18}F-FET-PET/CT were considered for inclusion. Patients were treated and examined from 2011, when Cyberknife treatment started in our hospital, to 2017, when dynamic parameter acquisition was discontinued. The diagnosis and histology before RRS were based on biopsies from metastatic sites or primary tumors. For the differentiation of tumor recurrence versus radiation necrosis after RRS, histopathology was used as reference diagnosis, if applicable. Else, the best supportive evidence using clinical and imaging data was used to determine reference diagnoses, like it was done in previously published studies [19,20,23]. Tumor recurrence was assumed when clinical symptoms related to the respective brain area occurred during follow-up and/or when the treated area became enlarged in imaging follow-up after treatment, defined as a >25% increase in the contrast-enhanced T1-weighted MRI scan according to MacDonald's criteria [30]. Radiation necrosis was diagnosed when neurological symptoms were constant

or improved over time and initially observed imaging changes in the treated area remained stable and/or became smaller. Retrospective reading was done by a neurosurgeon specialized in RRS and a nuclear medicine specialist, each with >10 years of experience. For the three patients still alive at the time of the study, reference diagnoses were determined 2 to 3 years after the PET examinations. In patients with multiple lesions, only the suspicious lesions that were the cause for referral to RRS were included in our retrospective analysis. Lesions with no tracer avidity in PET were excluded from quantitative analysis.

2.2. Robotic radiosurgery (Cyberknife®), MRI and ^{18}F-FET-PET/CT

Treatment of brain tumors was performed with the CyberKnife® VSI Robotic Radiosurgery System (Accuray, Inc., Sunnyvale, California, USA). The planning target volume (PTV) was defined as the gross tumor volume (GTV) based on contrast-enhanced CT (0.75 mm slice thickness) and co-registered cMRI (contrast-enhanced T1-weighted fast three-dimensional gradient-echo images), with a 0, 1 mm safety margin added. RRS treatment planning was performed using MultiPlan (Version 4.5, Accuray Inc., Sunnyvale, CA). For all brain lesions included, the dose was administered in a single session.

Most patients underwent follow-up cMRI on an outpatient basis using a standard protocol with a head coil at 1.0, 1,5, or 3.0 Tesla. Standard sequences included precontrast T2- and T1-weighted sequences and a T1-weighted postcontrast sequence along with thin-sliced (1 mm) three-dimensional isovoxel gradient echo sequences for multiplanar reconstruction.

Dynamic ^{18}F-FET-PET/CT was performed using Philips Gemini TF 16" with Astonish TF-Technology (Philips Healthcare, Eindhoven, The Netherlands). Patients were fasting or on a low-protein diet for 4–6 h before imaging. The 40-min emission scan was started after intravenous ^{18}F-FET injection (150-200 MBq). Dynamic PET data were acquired in List mode. PET images were acquired with a 16 cm axial field of view in a bed position with the skull base at the center. Images were reconstructed using a 128 × 128 matrix. Reconstruction was done manually with the filter set to "normal". Dynamic data were reconstructed into 20 frames with predetermined durations (6 × 20 s, 8 × 1 min and 6 × 5 min). Attenuation correction was enabled using a low-dose CT scan (5 mm slice thickness, 30 mAs current, 120 kV voltage, 0.5 sec gantry rotation time, 512 matrix size).

2.3. Variables

Static and dynamic PET parameters of each lesion were determined by the senior author, V.P., from semiautomatically drawn regions of interest (ROIs) placed in suspected lesions and normal brain tissue using a 40% isocontour threshold. V.P. was blinded to the patients' follow-up course and reference diagnoses of the lesions analyzed. Parameters included mean and maximum tumor-to-background ratios (TBR), calculated using mean and maximum standard uptake value (SUV) of lesions measured at 30–40 min after injection divided by the respective SUV of normal brain – with SUV defined as tissue radioactivity divided by radioactivity per gram of body weight –, time-to-peak (TTP), which was defined as the interval from the start of the dynamic acquisition to the time of maximum SUV, as well as time-activity curve (TAC), which depicts the time course of lesion SUV over the course of acquisition. There are three generally accepted tracer uptake patterns originally described for glioma grading: TAC I for ascending curve, TAC II for plateau, and TAC III for descending curve [31], which mirror uptake characteristics of lesions as follows: TAC I indicates non-tumorous lesions while tumorous lesions with high metabolism tend to have TAC II or III patterns.

Qualitative analysis was performed for lesions with suspicious MRI morphology but without visible ^{18}F-FET-tracer uptake in PET analysis.

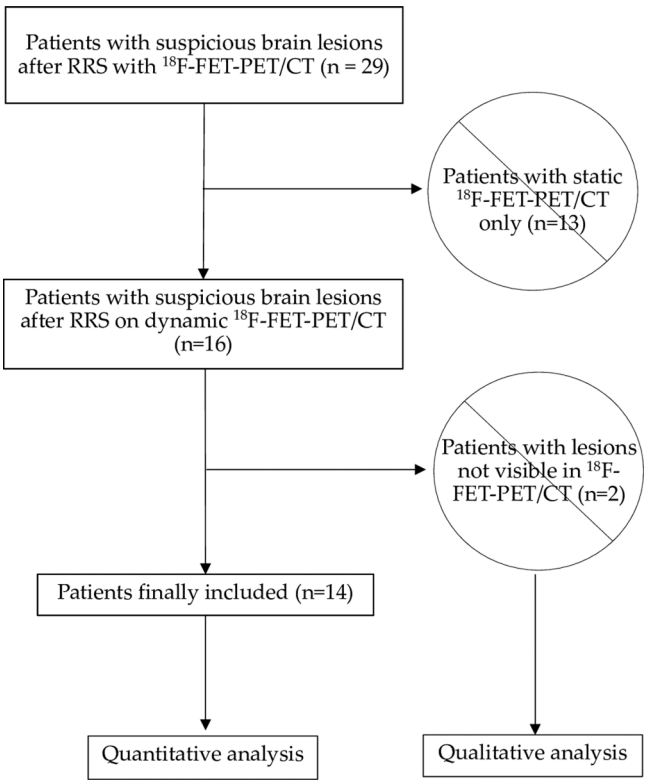

Fig. 1. Patient recruitment flowchart. RRS = robotic radiosurgery, ^{18}F-FET-PET/CT = (O-(2-[^{18}F]-fluoroethyl)-l-tyrosine positron emission tomography/computed tomography.

2.4. Statistics

PET parameters were analyzed for primary and secondary brain lesions taken together (TOTAL) and for the subset of metastatic brain lesions (METS). Descriptive analyses are shown with numbers and percentages or means, standard deviations, medians and ranges. Statistical analyses were performed using SPSS Statistics (Version 24, IBM, Armonk, NY, USA).

Data were tested for normal distribution. The Kruskal-Wallis test with post-hoc testing was performed to evaluate group differences of dynamic parameters as an orientation. In this retrospective exploratory study, no sample size calculation was performed beforehand. Confidence intervals were calculated for estimated parameters. Due to the explorative nature of the study, no adjustment for multiple testing was made for the different hypotheses (besides post-hoc tests).

Receiver-operating-characteristics (ROC) curves were generated with the aim to establish thresholds for ^{18}F-FET-PET/CT parameters. However, due to the small study population, no reliable thresholds could be established. Published thresholds closest to the results derived from our ROC analyses were thus used as cut-offs for diagnostic accuracy testing: TBR_{mean} of 1.95 and TTP of 20 min [19,20,23]. Diagnostic test accuracy was analyzed for all static and dynamic ^{18}F-FET-PET/CT parameters alone and in combination: sensitivity, specificity, and Youden's J statistic (Youden index) were calculated. Crude accuracy was defined as the sum of true positives and true negatives divided by all positive and negative counts [32,33].

As ^{18}F-FET-PET/CT is not used as the only diagnostic imaging test in patients, but as second-line imaging modality after initial MRI, pre-/posttest probabilities were calculated as the main outcome measure of this study: pretest probability was the baseline diagnostic probability using MRI alone compared with the reference diagnosis. Posttest probabilities were calculated using different ^{18}F-FET-PET/CT parameters. Relative differences (in percentage points, p.p.) between baseline pre-

Table 1
Study population characteristics (a) and time intervals (b).

(a)

Sex		2 (14%) males / 12 (86%) females	
Age		median 52 years; range 16-79 years	
Number of brain lesions per patient		**Number of patients (percentage)**	**Number of lesions (percentage)**
1		3 (21.4)	3 (10.7)
2		9 (64.3)	18 (64.3)
3		1 (7.1)	3 (10.7)
4		1 (7.1)	4 (14.3)
Total		14 (100)	28 (100)
Histology		5 (36)	7 (25)
WBRT before RRS		6 (43)	13 (46)
Diagnosis		**Number of patients (percentage)**	**Number of lesions (percentage)**
Primary brain tumor	Ependymoma	1 (6.67)	3 (10.34)
	PTPR	1 (6.67)	2 (6.90)
Brain metastasis	Breast cancer	9 (60)	18 (62.07)
	Non-small-cell lung cancer	2 (13.33)	3 (10.34)
	Malignant melanoma	1 (6.67)	2 (6.90)
Total		14 (100)	28 (100)

Note: Three non-avid lesions (metastasis from breast and lung cancer) are not included in the table.

Systemic Therapy During or Prior to PET-Time	**Number of patients (percentage)**	**No. of Radiation Necrosis (percentage)**	**No. of Recurrent Tumor (percentage)**
None	8 (28.6)	6 (75)	11 (55)
Antibody	3 (10.7)	0 (0)	6 (30)
Chemotherapy	3 (10.7)	2 (25)	3 (15)
Total	14 (100)	8 (100)	20 (100)

(b)

Time intervals (months)	**Mean (SD)**		**Median**		**Range**	
	TOTAL	**METS**	**TOTAL**	**METS**	**TOTAL**	**METS**
WBRT to RRS		16.27 (9.1)		12.70		8.28-33.58
Last RRS to ^{18}F-FET-PET/CT	12.96 (7.3)	11.46 (5.8)	10.00	9.00	4-35	4-23
Last MRI to ^{18}F-FET-PET/CT	0.55 (0.2)	0.51 (0.3)	0.49	0.49	0.23-1.02	0.23-1.02
WBRT to ^{18}F-FET-PET/CT	25.43 (16.1)	29.25 (8.6)	28.16	29.26	2.3-47	16.95-40.18

WBRT = whole-brain radiotherapy, RRS = robotic radiosurgery, PTPR = papillary tumor of pineal region, SD = standard deviation, ^{18}F-FET-PET/CT = dynamic (O-(2-[^{18}F]-fluoroethyl)-l-tyrosine positron emission tomography/computed tomography, MRI = cranial MRI follow-up, TOTAL (n=28) includes all primary and secondary brain tumors. METS (n=23) includes only brain metastases

and posttest probabilities were defined as the improvement made in diagnostic probability and were used as measures of the diagnostic quality of the ^{18}F-FET-PET/CT parameters.

3. Results

3.1. Patient/Lesion characteristics

Fig. 1 depicts the flowchart of patient recruitment. Fourteen patients (2 males, 12 females) with a median age of 52 years (range 16–79 years) and a total of 28 brain lesions were included (Table 1a). The majority of patients (80%) had brain metastases, accounting for a total of 23 lesions; only 5 lesions in two patients were primary brain tumors. The most common primary tumor site in the case of brain metastases was breast cancer (60%). Histology was available for only seven lesions, of which 14% were radiation necrosis. Thirty-three percent of the remaining 21 lesions were radiation necrosis based on expert assessment. We also assessed the systemic treatment of the patients. Eight patients did not have any systemic therapy during or prior to the PET scan. Six patients were undergoing systemic therapy during or prior to (2,3 months) the PET scan, three each with antibody (bevacizumab or trastuzumab emtansine), and chemotherapy (gemcitabine, pemetrexed, carboplatin).

All lesions were treated with single-session RRS using a prescription dose range of 13–20 Gy with a comparable median planning target volume (PTV) and gross tumor volume (GTV) of 1.5 cm^3 (Table S1). Four lesions (corresponding to 16.7% in TOTAL, 17.4% in METS) were treated twice with RRS prior to dynamic PET. In these cases, the median interval between the two sessions was 58 weeks with a mean of 54 weeks (range 27.6–70.9 weeks). Primaries of these four lesions were malignant melanoma, lung cancer, and breast cancer.

Six patients with a total of 13 lesions were treated by whole-brain radiotherapy (WBRT) prior to RRS. The median interval between WBRT and RRS was 12.7 months with a range of 8.3–33.6 months. After RRS, progressive enhancement led to PET examination after mean

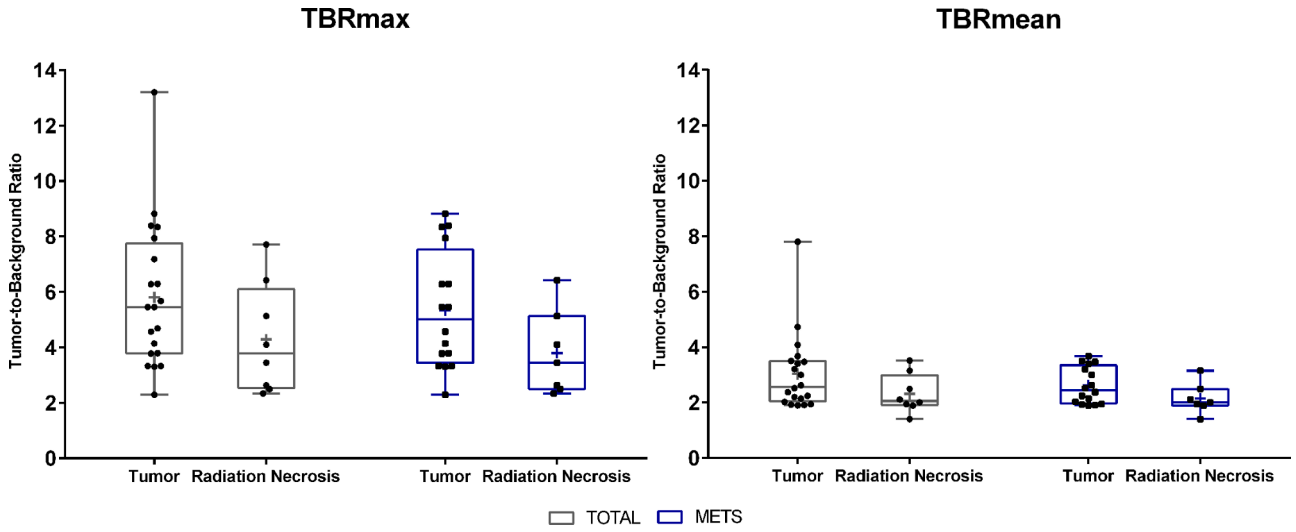

Fig. 2. Descriptive analyses of value distribution of TBRmax and TBRmean in recurrent tumors vs. radiation necrosis in both TOTAL (n = 28) and METS (n = 23) groups. Mean TBRmax: 5.8 (95% CI: 4.6 - 7.0) vs. 4.3 (95% CI: 2.6 - 5.9) in TOTAL and 5.3 (95% CI: 4.2 - 6.5) vs. 3.8 (95% CI: 2.4 - 5.2) in METS. Mean TBRmean: 3.0 (95% CI: 2.4 - 3.7) vs. 2.3 (95% CI: 1.7 - 2.9) in TOTAL and 2.6 (95% CI: 2.3 - 3.0) vs. 2.1 (95% CI: 1.6 - 2.6) in METS. Median TBRmax: 5.5 vs. 3.8 in TOTAL and 5.0 vs. 3.5 in METS. Median TBRmean; 2.6 vs. 2.1 in TOTAL and 2.4 vs. 2.0 in METS. Whiskers = range in min-max; + = mean; midline = median; dots and squares = individual data points in TOTAL and METS, respectively.

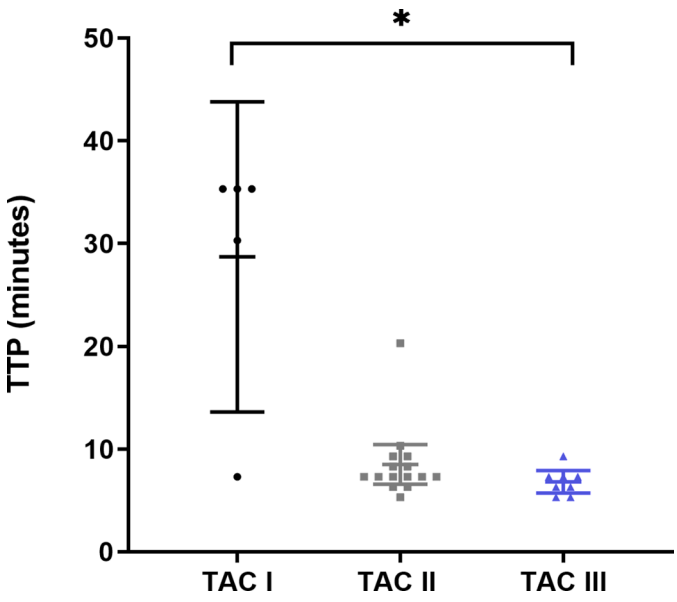

Fig. 3. Relationship between TAC patterns and TTP. Pairwise comparisons of TTP differences among TAC patterns. The Kruskal-Wallis test (Dunn correction) was performed for all lesions. Scatter plots depict mean and 95% CIs. Dots, squares, and triangles are individual data points of TTP distribution in TAC I, II, and III respectively. * p = .004, TAC I-II; p = .068, TAC II-III; p = .44 with mean ranks of 23.7 for TAC I, 14.27 for TAC II, and 9.2 for TAC III.

intervals of 11 and 13 months and median intervals of 9 and 10 months (METS and TOTAL, respectively); in one patient with brain metastasis, the interval was only 4 months (Table 1b).

3.2. Quantitative analysis

We analyzed tumor-to-background ratios (TBR) to determine their distribution in TOTAL and METS groups (Fig. 2). TBR tended to be higher in RT than in RN: median TBR_{max} of 5.5 vs. 3.8 in TOTAL and 5.0 vs. 3.5 in METS; and median TBR_{mean} of 2.6 vs. 2.1 in TOTAL and 2.4 vs. 2.0 in METS.

Relationships between TTP and TAC patterns were analyzed. A significant difference was only seen between TAC I and TAC III for all lesions with medians of 35.3 min for TAC I vs 6.8 min for TAC III and means of 28.7 min for TAC I vs. 6.8 min for TAC III. Other pairwise comparisons (TAC I vs. TAC II and TAC II vs. TAC III) did not reveal significant differences (Fig. 3). Mean TTP was shorter in tumors than in radiation necrosis: 9.6 vs. 16.7 min in TOTAL and 8.3 vs. 13.7 min in METS, while median TTP values did not differ (Table S2).

No significant TBR and TTP thresholds could be determined in our ROC analyses. Thus, published cut-offs for TBR_{mean} of 1.95 and for TTP of 20 min were chosen for the diagnostic accuracy tests as described in the Methods section [19,20,23]. Accuracy and the trade-off relationship of sensitivity and specificity calculated with Youden's J were best when only TAC was used, however, with a specificity of merely 50% (Table 2). Specificity was higher when static and dynamic PET parameters were combined, TBR_{mean}+TAC: 63%) (Table 2). Compared with cMRI as baseline (pretest), the probability of making a correct diagnosis was increased by only 5 p.p. when static ^{18}F-FET-PET parameters were used. When static and dynamic parameters were combined, a relative improvement in diagnostic probability of 12 p.p. in TOTAL and of 16 p. p. in METS was achieved. The improvement in diagnostic probability achieved with combined static and dynamic parameters was highest when only TAC without TTP was used as a dynamic parameter (Table 2).

3.3. Qualitative analysis

There were three non-^{18}F-FET-avid brain lesions, which were excluded from quantitative analysis. These lesions were qualitatively assessed using available clinical and radiological information. Fig. 4 shows cMRI and PET findings in these lesions. While cMRI suggested progressive enhancement, there was no tracer avidity in ^{18}F-FET-PET/CT – consistent with benign changes. Subsequent cMRI after PET confirmed regression or stable size of the lesions.

4. Discussion

4.1. Summary

Cyberknife stereotactic robotic radiosurgery has submillimeter precision as it allows real-time adjustment when the patient moves during

Table 2
Diagnostic test accuracy. Diagnostic accuracy parameters (sensitivity, specificity, accuracy with 95% CIs) for PET parameters and their combinations along with their corresponding diagnostic post-test probabilities.

	Baseline (cMRI)								Test Odds / Diagnostic Probability (%)	
	SE (95% CI)		SP (95% CI)		Youden's J		ACC (95% CI)		TOTAL	METS
	TOTAL	METS	TOTAL	METS	TOTAL	METS	TOTAL	METS	2.5 / 71%	2.3 / 70%
TBRmean	80% (56-94)	75% (48-93)	38% (9-76)	43% (10-82)	18%	18%	68% (48-84)	65% (43-84)	3.2 / 76%	3.0 / 75%
TTP	95% (75-100)	94% (70-100)	38% (9-76)	29% (4-71)	33%	23%	79% (59-92)	74% (52-90)	3.8 / 79%	3.0 / 75%
TAC	**95% (75-100)**	**100% (79-100)**	**50% (16-84)**	**57% (18-90)**	**45%**	**57%**	**82% (63-94)**	**87% (66-97)**	**4.75 / 83%**	**5.3 / 84%**
TBRmean+TAC	75% (51-91)	75% (48-93)	**63% (24-91)**	**71% (29-96)**	38%	46%	71% (51–87)	74% (52-90)	**5.0 / 83%**	**6.0 / 86%**
TBRmean+ TAC + TTP	**90% (68-99)**	**94% (70-100)**	50% (16-84)	57% (18-90)	**40%**	**51%**	**79% (59-92)**	**83% (61-95)**	4.5 / 82%	5.0 / 83%

cMRI = cranial magnetic resonance imaging, SE = sensitivity, SP = specificity, ACC = accuracy, CI = confidence interval, TBR = tumor-to-background ratio, TTP = time-to-peak, TAC = time-activity curve. TOTAL ($n = 28$) includes all primary and secondary brain tumors. METS ($n = 23$) includes only brain metastases. Annotations: Youden's J statistic = Sensitivity + Specifity - 1; bold print: highest values for single tests and combinations

treatment [5,6] and non-isocentric radiation contribute to more inhomogeneous and conformal dose distribution compared with other SRS systems [34,35]. However, RRS technology is not widely available worldwide, and its radiobiological mode of action is still unclear [10, 11]. Recently, an experimental mouse model was established to study radiation biology after RRS with first insights into early effects [36]. More research and experience are needed to understand the exact mode of action of RRS in order to be able to draw translational conclusions. Therefore, analysis of clinical data can make an important contribution. To our knowledge, this study is the first to assess the feasibility and benefit of dynamic ^{18}F-FET-PET/CT in differentiating tumor recurrence from radiation necrosis in the follow-up of RRS-only patients.

4.2. Key findings

In our patient population, the time intervals between RRS treatment and PET examinations were > 6 months in all but one case, reducing the likelihood of self-limiting posttherapeutic changes. The only exception was a case of breast cancer metastasis with an interval of only 4 months; tumor recurrence of this lesion was confirmed by biopsy in the further course of disease.

In our analysis of ^{18}F-FET-PET parameters as one diagnostic component, sensitivity was highest for TAC alone, followed by combinations of two (TBR_{mean} and TAC) and three parameters (TBR_{mean}, TAC and TTP) in the brain metastasis group. TAC alone showed the highest Youden's index but at the cost of specificity. The combination of TBR_{mean} and TAC showed a better specificity at the cost of sensitivity. However, for differentiating RT from RN, diagnostic probability is best when combining the two static (TBR_{mean}) and the dynamic (TAC) parameter (12 to 16 p.p. increase versus 5 p.p. for static PET alone). Therefore, combined static and dynamic PET is justified in clinical routine as time-activity curves provide relevant additional information for tumor characterization: higher amino acid metabolism within tumors causes rapid and higher tracer uptake compared to other lesions such as radiation necrosis, which tend to have slower or no uptake. We found malignant lesions to have higher tumor-to-background ratios and shorter time-to-peak, consistent with previously reported findings (Table S3). We emphasized that these results were reached using cut-off values of TBR_{mean} of 1.95 derived from other studies (TBR_{mean} 1.95 has been successfully reproduced in 3 previously published studies [19,20, 23]), and a TTP threshold of 20 min, which was closest to our own nonsignificant TTP cut-off of 25 min, hence allowing an indirect proof of concept of these published cut-offs on our study population. The readers assessing individual parameters (TBR_{mean}, TAC, or TTP) were not blinded to the results achieved with the combined parameters. All analyses were separately performed for all brain tumors and for brain metastases alone to allow reasonable comparison with published data, which mainly included either only gliomas or only metastases. Since there were only five primary brain tumors in two patients in our study population, no separate analysis for this group was performed.

Unlike other studies that investigated the same issue in patients after SRS, we achieved only moderate results (Table S3). Other studies report sensitivities of up to 95% and specificities of up to 93% with pooled sensitivity of 83% and pooled specificity of 89% for differentiation of brain metastasis from radiation necrosis [22]) or sensitivities of 80-100% and specificities of 75–100% for differentiation of glioma from radiation necrosis (Table S3). Only Guffens et al. reported a low sensitivity of 69% [21]. A possible explanation is that there was great homogeneity in metastatic tumor entities in our study: sixty percent of our patients had brain metastases from breast cancer. This reflects the poor prognosis of metastasized breast cancer, particularly compared to lung cancer – another primary tending to metastasize to the brain [37–39]. Other feasible explanations include the very small study population compared to other studies (Table S3) and the effect of technical differences between RRS and other methods of radiotherapy/-surgery, possibly resulting in more severe and prolonged local brain damage and, consequently, in a lower accuracy of ^{18}F-FET-PET/CT.

We compared the sensitivity and specificity results for lesions with versus without histological verification: we found that without histology, the sensitivity values were relatively constant (with the exception of TBRmean + TAC, here the sensitivity was remarkably lower than with histological verification), whereas the specificity became lower. In general, we can say, that the results for lesions without histological verification follow the patterns of results from the Table 2, but with constantly even lower specificity values. Thus, we postulate that the lack of histological verification is even more relevant for specificity values. In our study, TTP alone or in combination seemed to be able to provide good sensitivities. Thus, as well-known from other diagnostic tests, stepwise diagnostic procedures can help to achieve good diagnostic results: when first a very sensitive test is applied, followed by a second test with high specificity, diagnostic results can be optimized.

Furthermore, our findings suggest that two TAC patterns instead of three could be sufficient and simplify interpretation of dynamic PET results. Finally, the absence of any ^{18}F-FET uptake in suspicious lesions on cMRI after RRS could also serve as an imaging biomarker for differentiating radiation necrosis from tumor recurrence.

4.3. Limitations and perspectives

Major limitations of this study are the small number of patients, its retrospective and single-center design, 60% of brain metastases originating from breast cancer comprising the major part of the metastases

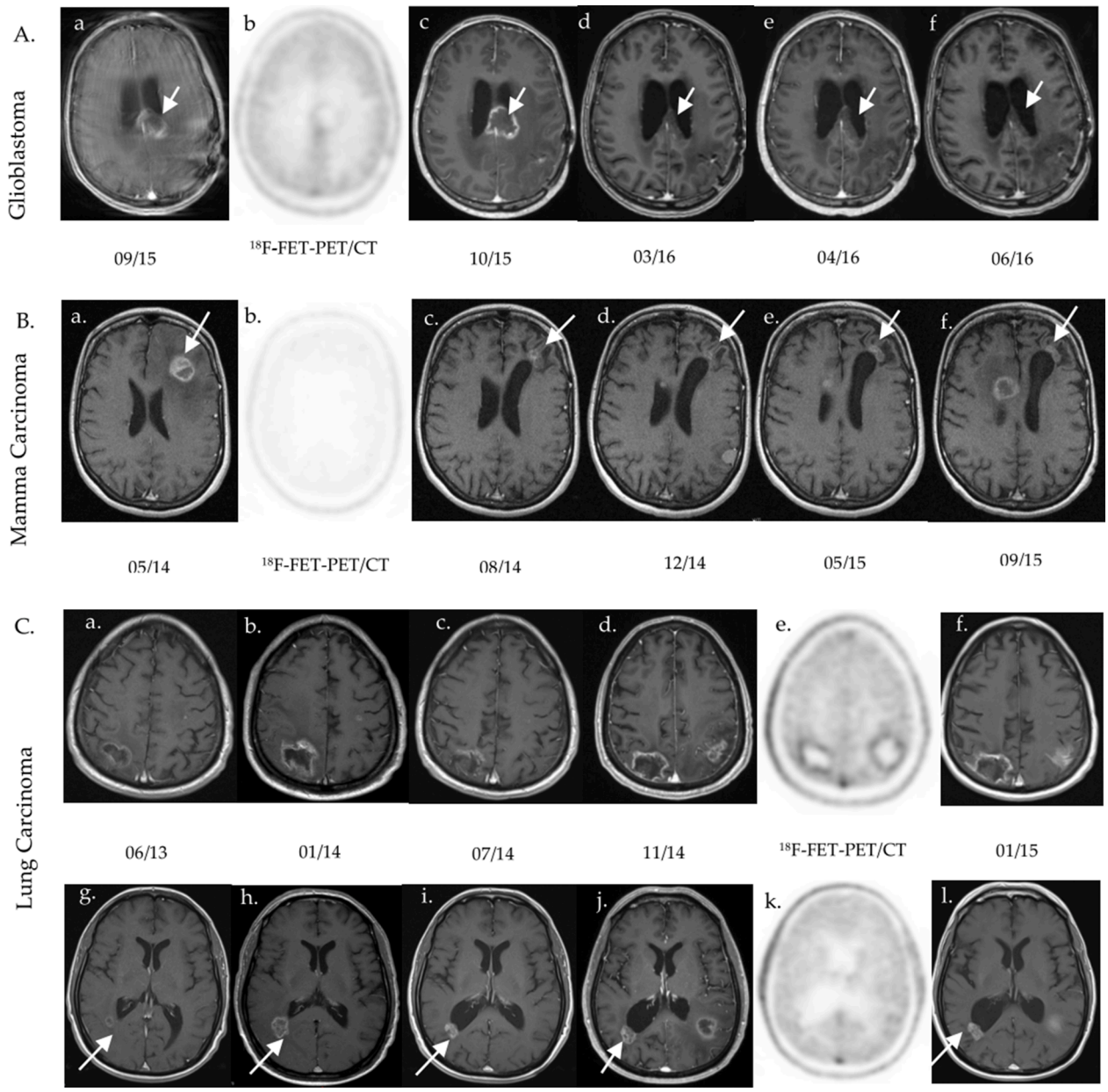

Fig. 4. Serial cMRI findings in three patients with non-^{18}F-FET-avid lesions. A and B are from two patients, each with a single suspicious brain lesion in cMRI (arrow) but without measurable correlation in PET (A(b) and B(b)). The follow-up shows a decrease in lesion size in one case (A) and a stable size in the other (B). Case C shows a patient with three suspicious lesions in cMRI (two parietal lesions in (a)-(f) and one right posterior horn lesion (arrow in g-l) treated in the same RRS session. In PET, the two parietal lesions (C(e)) show tracer uptake whereas the lesion near the right posterior horn does not (C(k)). In cMRI follow-up, the two parietal lesions in C(f) show an increase in size while the posterior horn lesion C(l) is stable.

group, and the lack of a control group. In addition, a histologic reference diagnosis was only available for few lesions, which is often the case in neuro-oncological studies because biopsy is not indicated for all lesions. Therefore, it is important to note that the results presented here are hypothesis-generating, as the combination of lack of histology as gold standard and the very small number of patients do not allow definite final conclusions to be drawn. The sample size in this study was small and could not be adapted for reasons of practical framework conditions.

Further, our data have a mix of independent and dependent characteristics (each lesion was used as an individual data point even though there were lesions that belonged to the same patient – another common practice in neuro-oncological studies, particularly with multiple brain metastases). This is why, for statistical testing, all comparisons would have to take into account independent and dependent observations and distributions, making statistical modelling cumbersome for small numbers. As this small pilot study provides first insights into this topic for RRS we hope that the experiences reported here can help other investigators in the planning of future larger studies and meta-analyses in this field and thus enable sample sizes that ease the use of such types of statistical models.

Future prospective studies should include sample size calculation and recruitment of patients with a clinical indication for ^{18}-F FET PET/CT with both static and dynamic parameter acquisition. If ethically and clinically possible, biopsy should be obtained in recruited patients after the PET scan to increase the quality of the diagnostic reference standard. Future studies should also be planned in accordance with methodological guidelines for diagnostic studies (e.g., blinded reading) and include analysis of interrater reliability.

Despite its limitations, this study is still of interest because it makes an important contribution toward the proof-of-concept of the diagnostic

potential of dynamic ^{18}F-FET-PET/CT in the clinical follow-up of RRS patients.

5. Conclusions

This single-center small explorative study provides initial insights into the diagnostic potential of dynamic ^{18}F-FET-PET/CT parameters in differentiating recurrent tumor from radiation necrosis after CyberKnife robotic radiosurgery with four pertinent findings:

- Combined static and dynamic ^{18}F-FET-PET parameters provide the best diagnostic accuracy in differentiating recurrent tumor from radiation necrosis.
- Dynamic PET parameters might have the potential to avoid unnecessary biopsies.
- Known ^{18}F-FET-PET/CT cut-offs from previous radiosurgery studies were applicable to CyberKnife patients.
- Two time-activity curve patterns (increasing and decreasing uptake) instead of the known three-pattern system may be sufficient to simplify image reading.

Funding

This research did not receive any specific grant from funding agencies in the public, commercial, or not-for-profit sectors.

Supplementary materials

Table S1. Robotic radiosurgery treatment characteristics, Table S2. TTP distribution of TAC patterns, Table S3. Compilation of studies investigating differentiation of radiation necrosis from recurrent brain metastases and gliomas.

CRediT authorship contribution statement

Winna Lim: Conceptualization, Methodology, Software, Formal analysis, Investigation, Data curation, Writing – original draft, Writing – review & editing, Visualization, Project administration. **Gueliz Acker:** Resources, Writing – original draft, Writing – review & editing, Supervision. **Juliane Hardt:** Methodology, Formal analysis, Investigation, Resources, Data curation, Writing – review & editing, Supervision. **Markus Kufeld:** Conceptualization, Formal analysis, Investigation, Writing – review & editing. **Anne Kluge:** Writing – review & editing, Supervision. **Winfried Brenner:** Writing – review & editing. **Alfredo Conti:** Resources, Writing – review & editing. **Volker Budach:** Resources, Writing – review & editing. **Peter Vajkoczy:** Resources, Writing – review & editing. **Carolin Senger:** Resources, Writing – original draft, Writing – review & editing, Supervision. **Vikas Prasad:** Conceptualization, Formal analysis, Investigation, Resources, Writing – review & editing, Supervision.

Declaration of Competing Interest

The authors declare that they have no known competing financial interests or personal relationships that could have appeared to influence the work reported in this paper.

Acknowledgments

The scientific data were in part obtained in the setting of the doctoral thesis of Winna Lim at Charité – Universitätsmedizin Berlin. Dr. Güliz Acker is a participant of the BIH-Charité Clinician Scientist Program funded by the Charité – Universitätsmedizin Berlin and the Berlin Institute of Health.

Supplementary materials

Supplementary material associated with this article can be found, in the online version, at doi:10.1016/j.ctarc.2022.100583.

References

[1] A.F. Eichler, et al., The biology of brain metastases-translation to new therapies, Nat. Rev. Clin. Oncol. 8 (6) (2011) 344–356.
[2] M.A. Vogelbaum, et al., Treatment for brain metastases: ASCO-SNO-ASTRO guideline, J. Clin. Oncol. 40 (5) (2022) 492–516.
[3] S.T. Chao, et al., Stereotactic radiosurgery in the management of limited (1-4) brain metastases: systematic review and international stereotactic radiosurgery society practice guideline, Neurosurgery 83 (3) (2018) 345–353.
[4] T. Nishizaki, et al., The role of cyberknife radiosurgery/radiotherapy for brain metastases of multiple or large-size tumors, Minim. Invasive Neurosurg. 49 (4) (2006) 203–209.
[5] S.D. Chang, et al., An analysis of the accuracy of the CyberKnife: a robotic frameless stereotactic radiosurgical system, Neurosurgery 52 (1) (2003) 140–146, discussion 146-7.
[6] L.N. Lohkamp, et al., Efficacy, safety and outcome of frameless image-guided robotic radiosurgery for brain metastases after whole brain radiotherapy, J. Neurooncol. 138 (1) (2018) 73–81.
[7] A. Muacevic, et al., Feasibility, safety, and outcome of frameless image-guided robotic radiosurgery for brain metastases, J. Neurooncol. 97 (2) (2010) 267–274.
[8] G. Acker, et al., Efficacy and safety of CyberKnife radiosurgery in elderly patients with brain metastases: a retrospective clinical evaluation, Radiat. Oncol. 15 (1) (2020) 225.
[9] N. Fatima, et al., The Stanford stereotactic radiosurgery experience on 7000 patients over 2 decades (1999-2018): looking far beyond the scalpel, J. Neurosurg. (2021) 1–17.
[10] C.W. Song, et al., Biological principles of Stereotactic Body Radiation Therapy (SBRT) and Stereotactic Radiation Surgery (SRS): indirect cell death, Int. J. Radiat. Oncol. Biol. Phys. 110 (1) (2021) 21–34.
[11] F. Gagliardi, et al., Role of stereotactic radiosurgery for the treatment of brain metastasis in the era of immunotherapy: a systematic review on current evidences and predicting factors, Crit. Rev. Oncol. Hematol. 165 (2021), 103431.
[12] J.M. Brown, D.J. Carlson, D.J. Brenner, The tumor radiobiology of SRS and SBRT: are more than the 5 Rs involved? Int. J. Radiat. Oncol. Biol. Phys. 88 (2) (2014) 254–262.
[13] E.K. Donovan, S. Parpia, J.N. Greenspoon, Incidence of radionecrosis in single-fraction radiosurgery compared with fractionated radiotherapy in the treatment of brain metastasis, Curr. Oncol. 26 (3) (2019) e328–e333.
[14] S.C. Thust, M.J. van den Bent, M. Smits, Pseudoprogression of brain tumors, J. Magn. Reson. Imaging (2018).
[15] G.C. Dooms, et al., Brain radiation lesions: MR imaging, Radiology 158 (1) (1986) 149–155.
[16] B. Vellayappan, et al., Diagnosis and management of radiation necrosis in patients with brain metastases, Front. Oncol. 8 (2018) 395.
[17] N.L. Albert, et al., Response assessment in neuro-oncology working group and European association for neuro-oncology recommendations for the clinical use of PET imaging in gliomas, Neuro. Oncol. 18 (9) (2016) 1199–1208.
[18] I. Law, et al., Joint EANM/EANO/RANO practice guidelines/SNMMI procedure standards for imaging of gliomas using PET with radiolabelled amino acids and [(18)F]FDG: version 1.0, Eur. J. Nucl. Med. Mol. Imaging 46 (3) (2019) 540–557.
[19] G. Ceccon, et al., Dynamic O-(2-18F-fluoroethyl)-L-tyrosine positron emission tomography differentiates brain metastasis recurrence from radiation injury after radiotherapy, Neuro. Oncol. 19 (2) (2017) 281–288.
[20] N. Galldiks, et al., Role of O-(2-(18)F-fluoroethyl)-L-tyrosine PET for differentiation of local recurrent brain metastasis from radiation necrosis, J. Nucl. Med. 53 (9) (2012) 1367–1374.
[21] M.A. F. Guffens, K. Van Laere, K. Goffin, A. Maes, Dynamic O-(2-18F-fluoro- ethyl)-l-tyrosine PET improves differentiation of local recurrent brain metastasis from radiation necrosis J. Nucl. Med. 56 (suppl 3) (2015) 628.
[22] H. Li, et al., Diagnostic accuracy of amino acid and FDG-PET in differentiating brain metastasis recurrence from radionecrosis after radiotherapy: a systematic review and meta-analysis, AJNR Am. J. Neuroradiol. 39 (2) (2018) 280–288.
[23] A. Romagna, et al., Suspected recurrence of brain metastases after focused high dose radiotherapy: can [18F]FET- PET overcome diagnostic uncertainties? Radiat. Oncol. 11 (1) (2016) 139.
[24] N. Galldiks, et al., Diagnosis of pseudoprogression in patients with glioblastoma using O-(2-[18F]fluoroethyl)-L-tyrosine PET, Eur. J. Nucl. Med. Mol. Imaging 42 (5) (2015) 685–695.
[25] N. Galldiks, et al., The use of dynamic O-(2-18F-fluoroethyl)-l-tyrosine PET in the diagnosis of patients with progressive and recurrent glioma, Neuro. Oncol. 17 (9) (2015) 1293–1300.
[26] S. Kebir, et al., Late pseudoprogression in glioblastoma: diagnostic value of dynamic O-(2-[18F]fluoroethyl)-L-Tyrosine PET, Clin. Cancer Res. 22 (9) (2016) 2190–2196.
[27] M.I. Mihovilovic, et al., O-(2-((18)F)fluoroethyl)-L-tyrosine PET for the differentiation of tumour recurrence from late pseudoprogression in glioblastoma, J. Neurol. Neurosurg. Psychiatry 90 (2) (2019) 238–239.

[28] W. Rachinger, et al., Positron emission tomography with O-(2-[18F]fluoroethyl)-l-tyrosine versus magnetic resonance imaging in the diagnosis of recurrent gliomas, Neurosurgery 57 (3) (2005) 505–511, discussion 505-11.
[29] P.M. Bossuyt, et al., STARD 2015: an updated list of essential items for reporting diagnostic accuracy studies, Radiology 277 (3) (2015) 826–832.
[30] D.R. Macdonald, et al., Response criteria for phase II studies of supratentorial malignant glioma, J. Clin. Oncol. 8 (7) (1990) 1277–1280.
[31] M.L. Calcagni, et al., Dynamic O-(2-[18F]fluoroethyl)-L-tyrosine (F-18 FET) PET for glioma grading: assessment of individual probability of malignancy, Clin. Nucl. Med. 36 (10) (2011) 841–847.
[32] A. Hoyer, A. Zapf, Studies for the evaluation of diagnostic tests-part 28 of a series on evaluation of scientific publications, Dtsch. Arztebl. Int. 118 (Forthcoming) (2021).
[33] C.E. Metz, Basic principles of ROC analysis, Semin. Nucl. Med. 8 (4) (1978) 283–298.
[34] G. Acker, et al., Image-guided robotic radiosurgery for treatment of recurrent Grade II and III meningiomas. A single-center study, World Neurosurg. 131 (2019) e96–e107.
[35] D. Kaul, et al., Dosimetric comparison of different treatment modalities for stereotactic radiosurgery of meningioma, Acta Neurochir. 157 (4) (2015) 559–563, discussion 563-4 (Wien).
[36] C. Jelgersma, et al., Establishment and validation of CyberKnife irradiation in a syngeneic glioblastoma mouse model, Cancers (Basel) 13 (14) (2021).
[37] H. Aoyama, Radiation therapy for brain metastases in breast cancer patients, Breast Cancer 18 (4) (2011) 244–251.
[38] J. Budczies, et al., The landscape of metastatic progression patterns across major human cancers, Oncotarget 6 (1) (2015) 570–583.
[39] F.G. Davis, et al., Toward determining the lifetime occurrence of metastatic brain tumors estimated from 2007 United States cancer incidence data, Neuro Oncol. 14 (9) (2012) 1171–1177.